

# Performance-Based Evaluation for Maximum Drag Reduction in HPHT Oilfield applications & systems

Joel Ulloa, Jamal Aamri, Basil Alfakher  
Saudi Aramco, Dhahran, Saudi Arabia

Sherif Tella  
Sinopec Middle East.

**Abstract - This study presents a performance-based testing methodology to evaluate five commercial high-viscosity friction reducers (HVFRs)—Xanthan gum, Guar gum, PHPA, PAC-LV, and Starch—at different concentrations using a pipeline friction loop system, HPHT acid-resistant rheometers, multi-sample stability Turbiscan Tower, and a surface tensiometer. Key parameters include drag reduction efficiency, flow rates, pressure drop, temperature stability, degradation resistance, and long-term performance under high-temperature and high-flow conditions. The study also investigates the impact of salinity on friction reducers and optimal concentrations to balance performance and stability. Xanthan gum, PHPA, and Guar gum outperform PAC-LV and Starch in drag reduction. Xanthan gum achieves 76% drag reduction at 0.5% concentration at low temperatures, while PHPA reaches 78% at 0.1% concentration at 158°F. Guar gum performs similarly to Xanthan gum but with lower efficiency. PAC-LV and Starch show poor performance, with Starch yielding negative rates and PAC-LV degrading at high temperatures. Rheological analysis reveals PHPA exhibiting better shear-thinning properties at 0.5% concentration. Higher concentrations expand the linear viscoelastic region in Xanthan gum and PHPA. Both maintain viscosity at elevated temperatures and effectively suspend proppants in static sand-settling tests. Salinity tests show Xanthan gum becomes unstable in monovalent ion brine but stabilizes at higher concentrations, while PHPA improves but destabilizes at increased concentrations. These findings guide better polymer selection for oilfield operations.**

**Keywords: Viscosity, Friction Reducers, Drag Reduction, Rheological Properties, Optimal concentration, salinity effects, and Proppant Carrying Capacity**

## Key Points

1. This study evaluates the drag reduction rate of polymers by measuring pressure drops across different pipeline sections. It assesses the effects of flow rates, concentrations, pipe diameters, and temperature on the drag reduction rates of each friction reducer.
2. Increasing polymer concentration does not necessarily enhance drag reduction rates, indicating an optimal concentration exists for each polymer.
3. All polymers exhibit pseudoplastic flow behaviour but saturate at different viscosity levels at high shear rates, with PHPA demonstrating strong shear-thinning properties at 0.5% optimal concentration and a broader viscoelastic region, ideal for maintaining flow and structure.
4. Xanthan gum and PHPA maintain viscosity at high temperatures and effectively suspend proppants, making them ideal for high-efficiency transport in oil and gas applications.
5. Salinity affects polymers differently: Xanthan gum destabilizes in monovalent ion brine unless concentration is increased while PHPA initially improves but becomes unstable at higher concentrations.

## 1. INTRODUCTION

Hydraulic fracturing, commonly known as fracking, is a widely utilized technique for extracting oil and natural gas from deep rock formations. It involves injecting high-pressure fluids composed of water, proppants, and chemical additives to create fractures within the reservoir, enhancing hydrocarbon recovery<sup>1,2</sup>. A critical component of fracking fluids is the friction reducer, which minimizes frictional resistance between the fluid and wellbore, improving fluid flow efficiency during injection<sup>3</sup>. Friction reducers play a key role in optimizing proppant transport, ensuring the newly formed fractures remain open and maximizing production rates<sup>4,5</sup>. Also in underground coal mines, the hydraulic fluid, mixed with a friction reducer, should reduce friction loss to maintain the hydraulic pressure while simultaneously discharging coal particles to clean the borehole<sup>6</sup>.

The selection of an appropriate friction reducer is vital, as improper choices can result in significant kinetic energy losses during fluid injection, leading to inefficient fracture propagation<sup>7</sup>. Additionally, incompatible or poorly formulated friction reducers can cause formation damage, which may impair permeability, reduce production rates, or render wells unproductive<sup>8,9</sup>. The concept of polymer-based friction reducers (FRs) was first introduced by Toms<sup>10</sup> in 1948, who observed that the addition of 10 mg/l of polymethylmethacrylate in monochlorobenzene could reduce frictional resistance by 30–40% at high Reynolds numbers. This ground-breaking discovery laid the foundation for the application of polymer FRs across various industries. The petroleum industry later adopted friction reducers to enhance oil transportation efficiency. The first large-scale application was implemented in the Trans-Alaska Pipeline System (TAPS) in 1979, where Poly-Alpha-Olefins were used as friction reducers. Their addition to the crude oil resulted in a 50% reduction in pressure losses, significantly increasing the pipeline capacity from 1450 to 2100 barrels per day<sup>11</sup>. Friction plays a significant role in fluid dynamics, particularly in pipeline systems, where the interaction between fluid molecules and pipe walls generates shear stress. This shear stress is influenced by fluid viscosity, velocity, and pipe surface roughness, which collectively increase pressure losses and energy consumption. To mitigate frictional losses, friction reducers are widely employed in hydraulic fracturing and pipeline operations, enhancing flow efficiency and prolonging equipment lifespan<sup>12</sup>. These additives reduce the drag forces between fluid molecules and the wellbore walls, leading to smoother flow and improved well productivity<sup>13</sup>. Mixed nonionic polymer/cationic surfactant system can significantly enhances turbulent drag reduction, especially at low polymer and high surfactant concentrations<sup>14</sup>. By modifying the viscosity and turbulence of the fluid, friction reducers help to prevent blockages and lower the need for high-pressure pumping, ultimately resulting in cost savings<sup>15,16</sup>. The drag reduction rate serves as a key parameter in evaluating friction reducers, as it directly impacts energy consumption, pressure drops, and overall operational costs. Effective friction reduction enhances operational efficiency, reduces downtime, and prolongs equipment lifespan, making it a critical factor in optimizing fluid flow in pipelines and wells<sup>17</sup>. Pipeline friction loop systems are commonly used to evaluate the drag reduction rates and performance of friction reducers, offering valuable insights into pressure drop reduction and degradation resistance over time<sup>18</sup>.

Rheological properties of friction reducers are essential for understanding their performance in oil and gas applications. These properties include viscosity, shear stress, and shear rate, which collectively determine the flow behavior of the fluid under varying conditions. The rheological properties and stability of MWCNTs/acrylamide polymer blends in harsh environments were studied<sup>19</sup>. It was observed that negative polyelectrolyte and polyampholytic polymers improve stability and viscosity at high salinity, temperature, and alkali conditions. However, the viscosity of friction reducers typically exhibits non-Newtonian behavior, where viscosity decreases with increasing shear rate (pseudoplastic behavior), enhancing fluid flow in turbulent regimes<sup>20,21</sup>. Shear-thinning properties are particularly advantageous in hydraulic fracturing, as they allow for easier pumping while maintaining proppant suspension<sup>22,23,24</sup>. Temperature and salinity can significantly influence the rheological behavior of friction reducers, affecting their efficiency and stability in different environments<sup>25,26,27</sup>. Understanding these properties enables engineers to optimize friction reducer formulations for specific applications, improving operational performance and reducing costs.

The performance of friction reducers in hydraulic fracturing operations is significantly influenced by various environmental factors, with salinity emerging as a critical parameter. High salinity levels, commonly found in produced water or formation water, pose substantial challenges to the efficacy of friction reducers. Produced water often contains dissolved salts such as sodium, chloride, calcium, and magnesium, with salinity levels varying based on geographic location, formation types, and extraction methods<sup>28,29</sup>. Elevated salinity alters the ionic strength of the fluid, affecting molecular interactions between friction reducers and fluid components. This can result in electrolyte screening effects that diminish polymer hydration, thereby reducing viscosity and friction reduction efficiency<sup>30</sup>. The impact of salinity on friction reducers extends to their stability and solubility, with ionic environments potentially causing conformational changes or polymer precipitation at high concentrations<sup>31</sup>. Some polymers exhibit better resilience to salinity, though others may require formulation optimization to maintain desired viscosities and friction reduction properties<sup>32,33</sup>. The reduced effectiveness of friction reducers in high-salinity environments can hinder proppant transport, impair fracture conductivity, and lower overall well productivity<sup>34,35</sup>. Consequently, understanding the interaction between salinity and

friction reducers is essential for optimizing hydraulic fracturing fluids in saline reservoirs, warranting continued research in this domain.

Understanding the performance and compatibility of friction reducers under varying downhole conditions is crucial for achieving optimal hydraulic fracturing outcomes. This study introduces a performance-based testing methodology to evaluate five different friction reducers based on drag reduction, rheological properties, and salinity performance. Current practices lack the capability to effectively assess the performance of friction reducers. The scope of this study focuses on the following aspects and experimental techniques:

1. **Pipeline Friction Loop System:** This system evaluates the drag reduction rate of polymers by measuring pressure drops across different pipeline sections. It assesses the effects of flow rates, concentrations, pipe diameters, and temperature on the drag reduction rates of each friction reducer.
2. **Rheological Properties Characterization:** This involves conducting tests such as linear and logarithmic shear rate ramp, amplitude sweep, frequency modulation, and ramp temperature sweep measurements. The performance index of the polymers is analyzed using parameters such as viscosity, shear rate, shear stress, yield stress, temperature, elastic modulus, storage modulus, and flow transition index.
3. **Salinity Influence Assessment:** This study examines the impact of monovalent ion brine (NaCl) on each polymer using four different approaches: multi-sample stability analyses, total dissolved solids (TDS) measurements, tensiometer testing, and rheological testing.
4. **Sand Settling/Proppant Carrying Capacity Tests:** The performance index of the friction reducers is also assessed using two types of tests: the single sand settling test and the sand ratio settling test.

## 2.0 MATERIALS AND METHODS

### 2.1 Selected Friction Reducers

This study presents a performance-based testing methodology to evaluate the effectiveness of five commercial high-viscosity friction reducers (HVFRs) — Xanthan gum, Guar gum, PHPA, PAC-LV, and Starch — across varying concentrations of 0.1%, 0.2%, 0.5%, and 0.8%. These friction reducers are derived from polysaccharides, polyacrylamide, and polyanionic cellulose, each possessing distinct molecular structures. Their molecular weight ranges between  $0.1 \times 10^7$  gmol<sup>-1</sup> and  $50 \times 10^6$  gmol<sup>-1</sup>, which significantly influences their drag reduction performance, stability, and rheological properties in fracturing fluids.

### 2.2 Experimental Lab Tests

#### 2.2.1 Rheological Measurement Tests

The rheological studies were conducted using both HTHP Ametek Chandler viscometer and HTHP acid-resistant MCR 302 rheometer equipped with different measuring systems. The measurements consist of the following tests: Linear and log shear rate ramp, amplitude sweep, frequency sweep and temperature ramp. These measurements help to identify fluid behavior under various flow conditions, allowing exploration of both low and high shear rates. They also provide insights into how polymers respond to applied stress or strain over time, revealing their time-dependent characteristics. Additionally, these measurements help to determine the transition between solid-like and liquid-like behavior and understand polymer behavior under different thermal conditions. The linear shear rate sweep is set to be  $0 \text{ s}^{-1}$  to  $170 \text{ s}^{-1}$  and the frequency backward sweep from  $500 \text{ rads}^{-1}$  to  $0.001 \text{ rads}^{-1}$ .

#### 2.2.2 Pipeline Friction Loop System

Another method for testing the friction reducers involves using pipeline friction loop systems as shown in **Figure 1**, which simulate the flow conditions of an actual pipeline. This controlled environment allows for the study of impact of flow resistance on friction reducers. The system comprises pipelines of various diameters, a pumping system, flowmeters ( $0.5 - 5 \text{ m}^3/\text{h}$ ), a pressure measurement system, a differential pressure measurement system ( $0 - 10 \text{ MPa}$ ), temperature control ( $0 - 302 \text{ }^\circ\text{F}$ ), a control system, a data acquisition system, a 50 L mixing tank, and a stirrer. The pipeline system includes inner diameters of 6 mm, 10 mm, and 12 mm, each with a length of 3 m. These diameters were selected to assess the effects of pipe size on frictional resistance. The flow rate of the pumping system varied from 0.5 to  $5.00 \text{ m}^3/\text{h}$  in  $0.250 \text{ m}^3/\text{h}$  increments. Initially, the system was calibrated with deionized water as the base fluid, and experiments were conducted at different temperatures with  $18 \text{ }^\circ\text{F}$  intervals.

The experimental procedures include setting up the test parameters from the interface software and running the system for a few minutes to ensure smooth fluid flow and no leakage. The flow rate and pressure are adjusted as needed to simulate different operating conditions. The test fluid is circulated through the loop system at a steady flow rate, and the flow rate, pressure, and temperature are monitored throughout the experiment. The pressure drop across the loop system is measured using pressure gauges or sensors at

both the inlet and outlet. Drag reduction rates are calculated using the pressure drop, flow rate, and other relevant parameters. The progress of the tests is monitored on the software interface.



Figure 1. Pipeline Friction Loop System

### 2.2.3 Salinity Measurement Tests

Stability, resilient in changes to salinity, effective hydrations and ionic strength of the polymers are some of the criteria to be considered for characterizing friction reducers and they play crucial roles in optimizing the fluid flow in pipelines and wells. The effects of monovalent brine on friction reducers will depend on the specific properties of the friction reducer and the concentration of the brine.

The salinity tests were conducted using Turbiscan Tower for stability analyses, TDS meter, force tensiometer, and HPHT rheometer to study the salinity effects of monovalent ion brine (NaCl) on the five friction reducers. The Turbiscan tower is used to evaluate the physical stability of the test solutions by monitoring changes in their microstructure over time and detect different types of instability phenomena such as sedimentation, creaming, flocculation, coalescence, or phase separation in real-time. The measurement procedures include ensuring test solution is homogeneous before taking samples and, if necessary, degas the sample to remove any air bubbles. Then, the Turbiscan sample cell is filled with the test solution to the appropriate level (around 20 mL). Prepare the cap stopper by inserting a seal to prevent leakage. and select the appropriate measurement parameters (e.g., measurement time, temperature) based on the test solution and desired analysis. The filled sample cell is placed in the Turbiscan Tower and begin the measurement process, which involves continuous monitoring of the sample using multiple wavelengths of light and capturing data on backscattering and transmission profiles across the height of the sample at predefined time intervals. These measurements focus on exploring the properties of polymers by examining factors like concentrations, and destabilization processes such as sedimentation, creaming, aggregation, and flocculation.

### 2.2.4 Proppant Carrying Capacity Tests

The performance of friction reducers is evaluated using the static sand settling test, consisting of the single sand settling test and the sand ratio settling test. In the single sand settling test, friction reducer fluids at different concentrations are prepared in a 100 mL graduated cylinder, and five 20/40-mesh quartz sands are added. The time taken for the sand to settle is recorded, and the average settling time is calculated. For the sand ratio settling test, 20/40-mesh sand is mixed with the fluid at a 150 kgm<sup>-3</sup> ratio, stirred at 500 – 1500 rpm for 5 – 15 minutes, and allowed to precipitate naturally. The tests provide insights into the stability of sand particles and the ability of the proppants to settle uniformly, which is essential for fracturing fluid applications.

## 3.0 RESULTS AND DISCUSSION

The friction reducers used in the analyses formed structured fluids and many factors can affect the stability of structured fluids. The viscosity and viscoelasticity of the liquid phase in dispersions typically influence the flow characteristics of the polymers. The molecular weight, concentration, temperature-dependent and attraction of the particles with the continuous phase in which they are suspended all affect their performance in the dispersions. In addition, Shearing can destroy this delicate structure and break down the fluids viscosity.

### 3.1 Rheological Measurements

#### 3.1.1 Viscosity and Flow Curves

All the polymer samples in these analyses exhibit pseudoplastic flow behaviour but saturate at different viscosity levels at high shear rates. In this case, the viscosity decreases as the shear rate increases. Pseudoplastic flow is often attributed to the orientation of

polymer chains as they align in the direction of the shear force. The viscosity and flow curves of 0.5% concentrations of all the polymers are shown in **Figure 2**.

The profile of the pseudoplastic behaviour is commonly referred to as shear thinning phenomenon. Shear thinning of polymers can be attributed to the structural changes that occur within the polymer when subjected to shear forces that determine the degree of easier fluid flow. As it can be observed from Figure 2 that the slope of PHPA is steeper than Xanthan Gum. Though, the high shear rate plateau of both polymers saturate at slightly the same level. Indicating that there is a gradual transition from low shear rate to high shear rate for Xanthan Gum compare to PHPA. However, the degree of shear thinning exhibited by a polymer depends on several factors, including the molecular weight, polymer concentration, temperature, and the specific chemical structure of the polymer. High molecular weight polymers and concentrated solutions tend to exhibit greater shear thinning behaviour compared to low molecular weight polymers or dilute solutions.

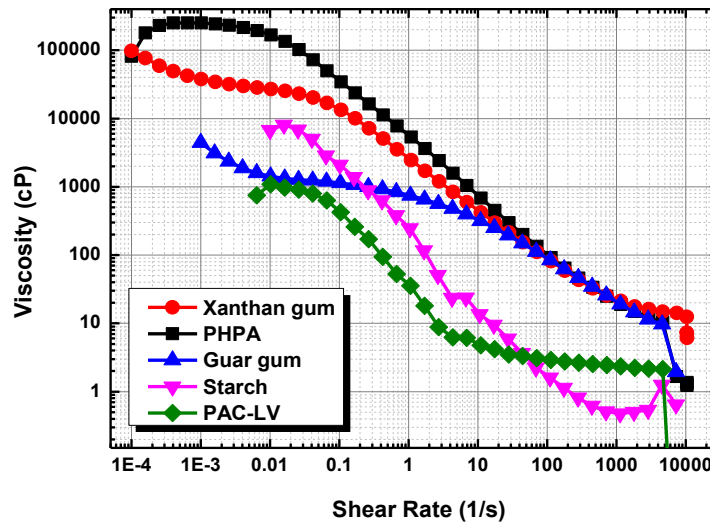


Figure 2. Flow curve and viscosity curve of 0.5% concentrations of all the polymers

The profile of the pseudoplastic behaviour is commonly referred to as shear thinning phenomenon. From these curves, two key aspects stand out: the shear thinning slopes that signify the shift from low shear rates to high shear rates, and the saturation of the high shear viscosity plateau, which can help determine the optimal viscosity range for friction reducers at high shear rates. Shear thinning of polymers can be attributed to the structural changes that occur within the polymer when subjected to shear forces that determine the degree of easier fluid flow. As it can be observed from **Figure 3**, the high shear viscosity plateaus are different for different concentrations and lead to different saturation levels. However, the optimal viscosity range for hydraulic fracturing is typically between 50 cP to 150 cP as low viscosity below 50 cP and high viscosity above 200 cP usually affect proppant transport and can also lead to issues such as increased pump pressure requirements, difficulty in fracture creation, and challenges in clean-up post-fracturing.

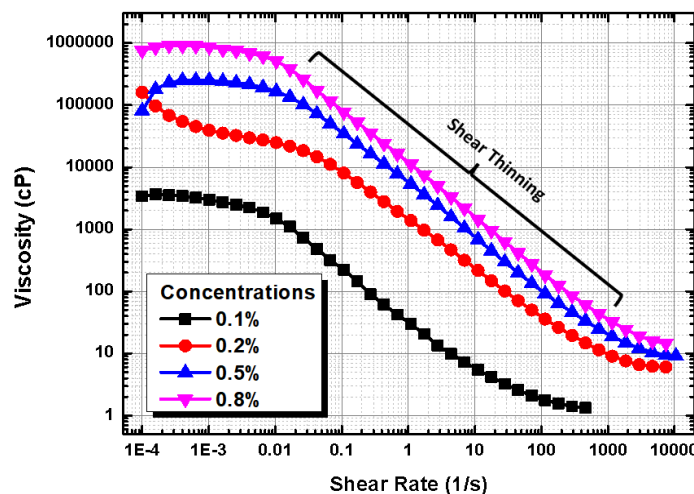


Figure 3. Viscosity curve for Xanthan Gum, presented on a logarithmic scale

### 3.1.2 Frequency Modulation Tests

Frequency sweep is a common technique used to analyse the viscoelastic properties of polymers. This technique is generally used to serve the purpose of describing the time-dependent behaviour of a sample in the non-destructive deformation range. This method involves subjecting the polymer sample to a range of frequencies and measuring the resulting mechanical responses. Frequency sweeps can provide important information about the molecular structure, cross-linking density, viscoelastic behaviour, and aging on the mechanical properties of the polymers. The profiles of the backward frequency sweep of 0.2% concentrations of PHPA is shown in **Figure 4** and 0.5% concentrations of Xanthan Gum and PHPA is shown in **Figure 5**.

It can be observed that there are two intersecting points between the storage and loss modulus. The loop domain represents the non-destructive deformation region for the polymers and it is used to evaluate the LVE (Linear Viscoelastic) region in the amplitude modulation profiles for each polymers. It can also be deduced that the loop domain is small for small concentrations and increases as the concentration increases for some polymers depending on the inner structure of the polymer. This indicates that for higher concentrations, the LVE region can be increased and the non-destructive deformation region increases respectively. The crossover point can be indicative of a transition in the behaviour of the polymers, providing insights into how the friction reducers will perform under different types of loading conditions.

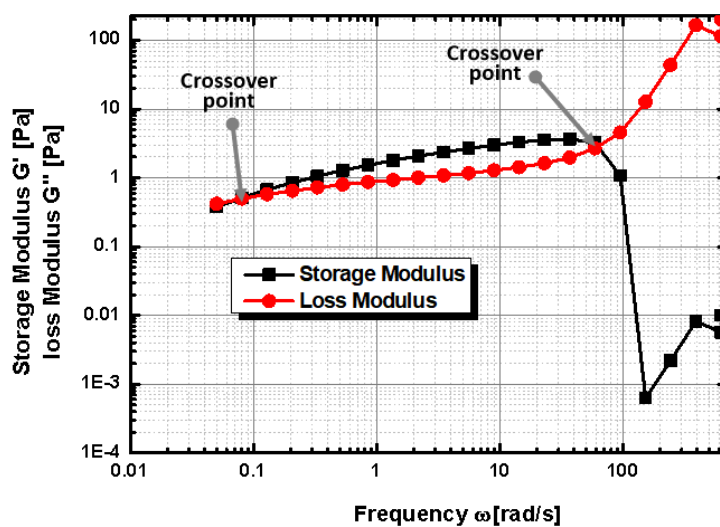


Figure 4. Frequency Modulation Curves for 0.2% concentration of PHPA

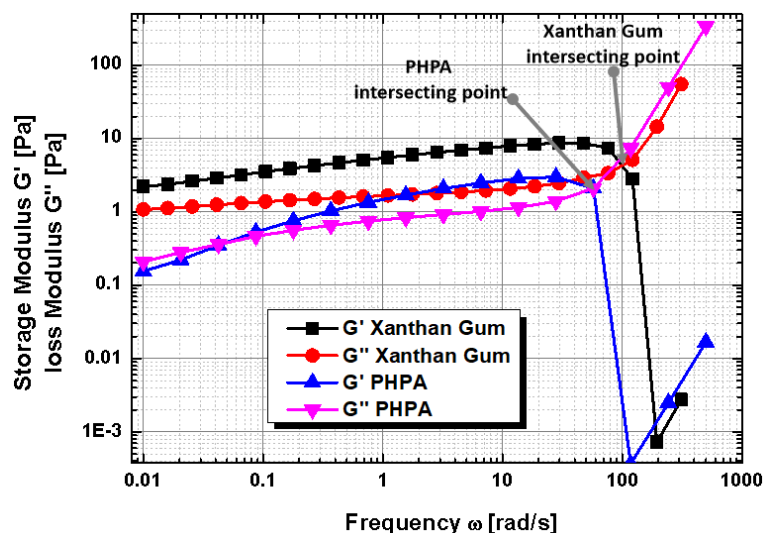


Figure 5. Frequency modulation curves for 0.5% concentration

### 3.1.3 Amplitude Modulation Tests

The amplitude sweep test is a rheological measurement technique used to characterize the viscoelastic properties of polymers. It involves subjecting the polymers to a sinusoidal stress or strain at different amplitudes and measuring the resulting response. This

technique can help to determine the range of strain or stress amplitudes within which the polymer exhibits linear viscoelastic behaviour and remains predominantly elastic. The frequency is typically kept constant throughout the test. In the case of these analyses, the frequency was kept constant at 1.6 Hz (10 rad/s) and 16 Hz (100 rad/s) which were obtained from the frequency sweep tests as aforementioned above. The two frequencies were selected based on the non-destructive and destructive deformation regions of the polymers.

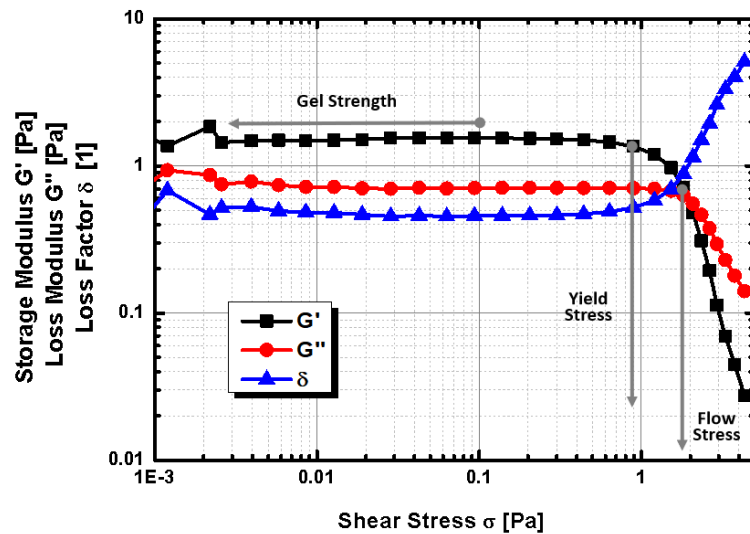


Figure 6. Amplitude modulation curves for 0.2% concentration of Xanthan Gum at frequency of 1.6 Hz (10 rad/s) presented with shear stress

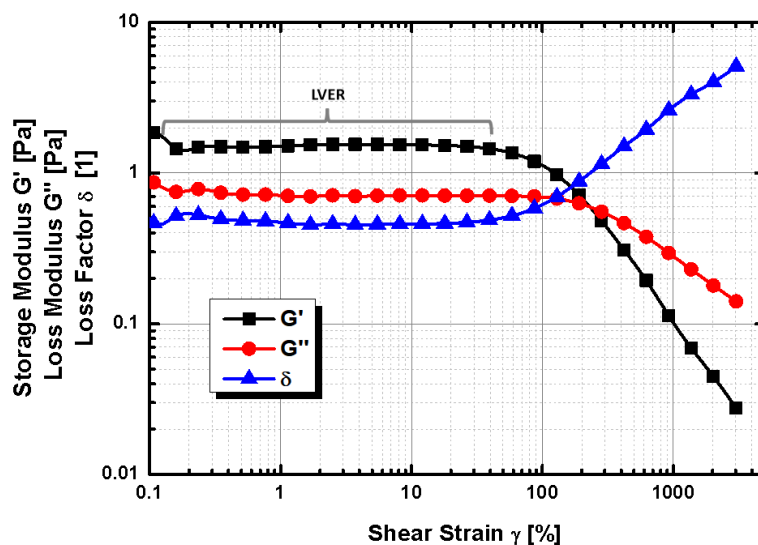


Figure 7. Amplitude modulation curves for 0.2% concentration of Xanthan Gum at frequency of 1.6 Hz (10 rad/s) presented with shear strain

The amplitude modulation curves for 0.2% concentration of Xanthan Gum at a constant frequency of 1.6 Hz with respect to the shear stress and shear strain are shown in **Figure 6** and **7**. The curve of the storage modulus is often preferred to determine the constant plateau value in the LVE region. These values are estimated to be 40% for Xanthan Gum. The gel strength, yield stress and flow stress are also estimated for the 0.2% concentration of Xanthan Gum to be 1.5 Pa, 0.9 Pa and 1.9 Pa respectively. The corresponding values for all other polymers at 0.2% concentration and 1.6 Hz frequency are shown in **Table 1** and **2**. However, the polymers were also tested at the frequency in the destructive deformation region to have insight about the viscoelastic behaviour of the polymers when sheared in this domain. The amplitude modulation curves for 0.2% concentration of Xanthan at a constant frequency of 16 Hz (100 rad/s) is shown in **Figure 8**.

Table 1. Performance evaluation parameters for 0.2% concentrations

Parameters	Polymers - 0.2% concentrations				
	A	B	C	D	E
LVER @ 1.6Hz (10 rad/s)	40%	50%	200%	30%	100%
LVER @ 16Hz (100 rad/s)	22.5%	1%	35%	0.8%	0%
Gel strenght (Pa)	1.5	2	0.075	0.2	0.035
Yield stress (Pa)	0.9	1	0.08	0.05	0.05
Flow stress (Pa)	1.9	4	0.18	0.2	0.09
Flow Transition index	2.1	4	2.25	4	1.8

Table 2. Performance evaluation parameters for 0.5% concentrations

Parameters	Polymers - 0.5% concentrations				
	A	B	C	D	E
LVER @ 1.6Hz (10 rad/s)	50%	100%	100%	7%	1%
LVER @ 16Hz (100 rad/s)	50%	50%	0.05%	1%	1%
Gel strenght (Pa)	6	10	0.35	2	0.025
Yield stress (Pa)	2.5	6	1	0.14	0.06
Flow stress (Pa)	8	10	0	0.5	0.095
Flow Transition index	3.2	1.7	0	3.5	1.6

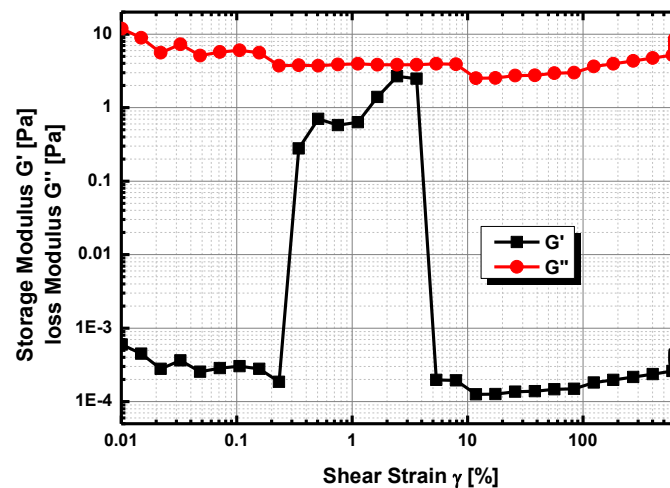


Figure 8. Amplitude modulation for 0.2% concentration of Xanthan Gum at frequency of 16Hz (10rad/s)

### 3.1.4 Implications for Dynamic Loading and Operational Stress

The pipeline friction loop tests, amplitude and frequency sweep tests provide valuable insight into how these polymers behave under dynamic flow conditions representative of real pipeline systems, which experience oscillatory shear, pressure surges, and fluctuating flow rates. The broad LVE regions observed for Xanthan Gum and PHPA indicate that these polymers can withstand cyclic shear without structural breakdown, maintaining elastic behavior over repeated deformation cycles. The absence of pronounced hysteresis or modulus degradation during backward sweeps suggests good structural resilience and minimal fatigue within the operational strain window.

Although creep-recovery and stress relaxation tests were not performed in the present study, the stable plateau moduli and predictable transitions from elastic to viscous regimes imply strong time-dependent recovery characteristics for Xanthan Gum and PHPA. These properties are essential for maintaining drag reduction efficiency and proppant carrying capacity during high-frequency pressure oscillations encountered in pumping operations.

In contrast, the small LVE regions and low gel strengths of Starch and PAC-LV indicate limited resistance to dynamic loading, explaining their tendency toward rapid viscosity loss and poor proppant suspension under operational stress. Incorporating full time-dependent rheological tests will be part of future investigations to quantify long-term structural stability and fatigue behavior.

### 3.1.5 Rheological Model Fittings

This study has considered and implemented rheological model fitting using the Power-Law (Ostwald–de Waele) model, which adequately describes the shear-thinning behavior observed in our polymer solutions. The Power-Law relationship is expressed as:

$$\tau = K\dot{\gamma}^n$$

Where:  $\tau$  is the shear stress,  $\dot{\gamma}$  is the shear rate,  $K$  is the consistency index, and  $n$  is the flow behavior index. The fitting was performed using a log–log regression approach, applying the formula:

$$\ln \tau = \ln K + n \ln \dot{\gamma}$$

Where the slope of the regression line provides the value of  $n$  and the intercept gives  $\ln K$ . This allowed model validation and comparison across polymer types and concentrations.

The fitted parameters  $n$  and  $K$  are summarized below for all polymer samples and concentrations. These parameters were extracted from the Power-Law regression model.

Table 3. Fitted parameters  $n$  and  $K$  for all polymer samples with varying concentrations

Polymers	0.1%		0.2%		0.5%		0.8%	
	$n$	$K$	$n$	$K$	$n$	$K$	$n$	$K$
Xanthan Gum	0.210	0.196	0.237	1.487	0.176	5.295	0.156	11.527
PHPA	0.333	0.573	0.276	1.242	0.284	2.561	0.235	3.385
Guar Gum	0.0267	0.0878	0.0359	0.0446	0.421	1.208	0.363	3.698
Pac LV	- 0.228	0.0887	- 0.0218	0.0562	- 0.137	0.033	0.185	0.0757
Starch	- 0.0119	0.173	- 0.156	0.104	- 0.0314	0.193	0.181	0.429

It can be observed that some values of flow behavior index are negative for PAC LV and Starch. A negative flow index implies that viscosity would approach infinity at low shear and collapse toward zero at high shear. Such behavior is physically unrealistic for stable polymer solutions and typically indicates that the Power-Law model is being applied outside its valid shear-rate range or that measurement artefacts (e.g., slip, low torque, or polymer degradation) are present. Therefore, negative  $n$  values are interpreted as non-physical and a sign of invalid data fitting rather than true fluid behavior.

The variation of rheological parameters with concentration shows clear differences among the polymers. Xanthan Gum demonstrated the strongest shear-thinning behavior, with sharply increasing consistency index ( $K$ ) and decreasing flow behavior index ( $n$ ), reflecting high viscosity and strong molecular interactions. PHPA also exhibited pseudoplasticity, though with more moderate increases in  $K$  and slight decreases in  $n$ . Guar Gum showed a mixed response, with both  $K$  and  $n$  increasing, suggesting progressive network development at higher concentrations. PAC-LV and Starch displayed irregular or nearly Newtonian trends, likely due to weaker molecular interactions or measurement sensitivity at low concentrations.

Overall, increasing polymer concentration generally led to higher  $K$  values and lower  $n$  values for most polymers, confirming enhanced shear-thinning as chain overlap and intermolecular interactions intensified. These trends highlight how polymer structure and concentration collectively govern flow behavior under shear.

This formulation enables the prediction of pressure losses, velocity profiles, and transport performance in pipeline and drilling operations. Consequently, it strengthens the practical relevance of our findings by allowing direct integration into process optimization strategies. By controlling the values of  $n$  and  $K$  through polymer concentration, operators can enhance proppant transport while minimizing frictional pressure losses, improve proppant suspension during hydraulic fracturing, and increase the carrying capacity of drilling fluids for cuttings, particularly under low-shear conditions.

### 3.1.6 Viscosity-Temperature Relationship

The viscosity of polymers is highly dependent on temperature. In general, as the temperature of a polymer increases, its viscosity decreases. This is due to the fact that at higher temperatures, the molecular motion and intermolecular forces within the polymer chains are increased, leading to a reduction in the resistance to flow. Some polymers may exhibit non-linear or even non-monotonic changes in viscosity with temperature, particularly if they undergo phase transitions or other complex behaviour. The viscosity-temperature curves for all the polymers are shown in **Figure 9** for 0.2% concentration. It can be noted that the profiles are the same for all the polymers and the viscosity decreases with increase in the temperature. As anticipated, higher temperatures lead to increased saturation levels with rising concentrations. Xanthan Gum and PHPA exhibit superior viscosity compared to others, while Starch and PAC-LV demonstrate significantly lower viscosities, even below that of water, at elevated temperatures. This suggests that Xanthan Gum and PHPA maintain more substantial viscous properties, whereas Starch and PAC-LV may not perform effectively in high-temperature scenarios.

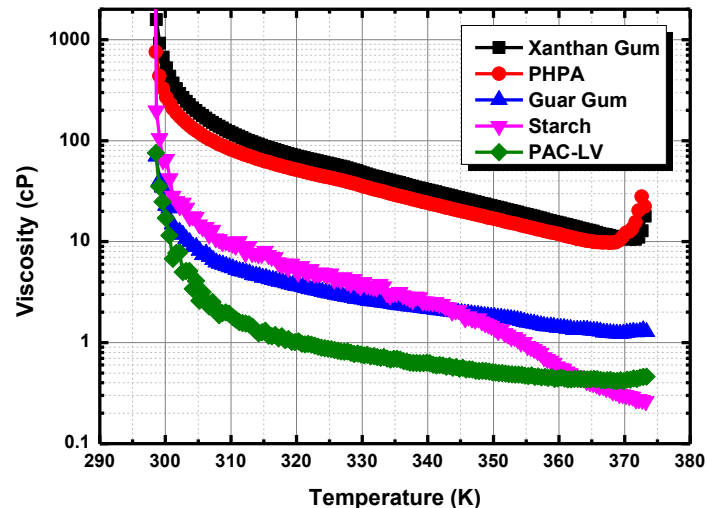


Figure 9. Viscosity-temperature relationships of all the polymers for 0.2% concentration

### 3.1.7 Influence of Polymer Molecular Structure on Rheological Behavior

The rheological performance of the polymers examined in this study is strongly governed by their intrinsic molecular architecture, including backbone rigidity, degree of branching, charge density, and hydrophilicity. Although the commercial products used did not include full FTIR, GPC, or zeta potential datasets, their structural characteristics are well established and help explain the pronounced differences observed in viscosity, shear thinning, gel strength, and LVE region behavior.

Xanthan Gum possesses a semi-rigid double-helical backbone with pyruvyl and acetyl substituents that introduce high anionic charge density. This rigidity, combined with electrostatic repulsion between carboxylate groups, promotes an extended conformation in solution and facilitates strong intermolecular interactions at low strain. This structural configuration explains the comparatively high gel strength, large LVE region, and significant yield stress values measured in the amplitude sweep tests.

PHPA, in contrast, is a flexible, coil-like polyacrylamide with a tunable degree of hydrolysis, containing both amide ( $-\text{CONH}_2$ ) and carboxylate ( $-\text{COO}^-$ ) groups. The partial anionic charge promotes moderate intermolecular repulsion, which increases chain extension but avoids the rigidity characteristic of Xanthan Gum. This flexibility enables PHPA to exhibit strong shear-thinning behavior, broad LVE regions at optimal concentrations, and high flow stress values. The high molecular weight of PHPA further contributes to the enhanced entanglement density and improved drag reduction performance observed at elevated temperatures. Guar Gum and Starch, both neutral polysaccharides dominated by hydroxyl-rich repeating units, form weaker viscoelastic networks because they lack significant electrostatic interactions. The galactose side branches of Guar gum increase hydration but do not generate sufficient chain repulsion to produce large elastic regions, resulting in lower gel strength and reduced yield stress. PAC-LV, a carboxymethylated cellulose derivative, exhibits moderate anionic character but significantly lower molecular weight and branching density, limiting both its entanglement ability and its viscoelastic contribution at low shear.

These structure-property relationships correspond directly to the viscoelastic parameters in Tables 1 and 2 and explain the superior rheological performance of Xanthan Gum and PHPA in applications requiring proppant suspension, thermal stability, and high drag reduction efficiency.

### 3.2 Sand Settling/Proppant carrying Capacity

The sand settling test is a technique employed to assess the settling properties of 20/40 mesh proppant within a heterogeneous mixture. This measurement helps assess how varying concentrations and viscosities impact the ability of the fluid to transport proppants. A slower rate of sand accumulation suggests a higher carrying capacity, which is essential during the stimulation process.

#### 3.2.1 Single Sand Settling Tests

Single sand settling tests are typically conducted to determine the settling characteristics of sand particles in a fluid. These tests are commonly used to assess proppants transport, sedimentation rates, and the behavior of sediments in various media. In the case of single sand settling tests as shown in **Figure 10**, it can be observed that the settling velocities are high in Guar Gum, Starch and PAC-LV. However, the settling velocities are low in both Xanthan Gum and PHPA. In fact, the proppants did not settle in 0.5% and 0.8% concentrations of their suspensions. Likewise, there is no proppant settlement in 0.8% concentration of Guar Gum. However, several factors may be responsible for the non-settlement of the proppants.

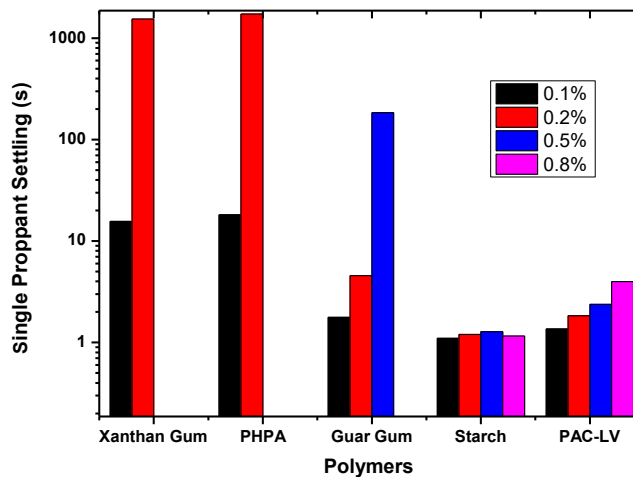


Figure 10. Settling rate for all concentrations of the polymers for single sand settling tests

#### 3.2.2 Sand Ratio Settling Tests

Sand ratio settling tests are typically performed to measure how the sand particles settle in a liquid medium, which can provide insight into particle size distribution, density, specific gravity, and the overall quality of the sand. **Figure 11** shows the settling rate of all the polymers. The sand carrying performance of 0.5% and 0.8% concentrations of Xanthan Gum were observed to be significantly higher than other polymers. All of the 20/40 mesh quartz sand settled at the bottom of other polymer in the sand ratio tests. However, it was only 90% of the proppants that settled in Xanthan Gum. Thus, Xanthan Gum has good static sand-carrying properties than other polymers.

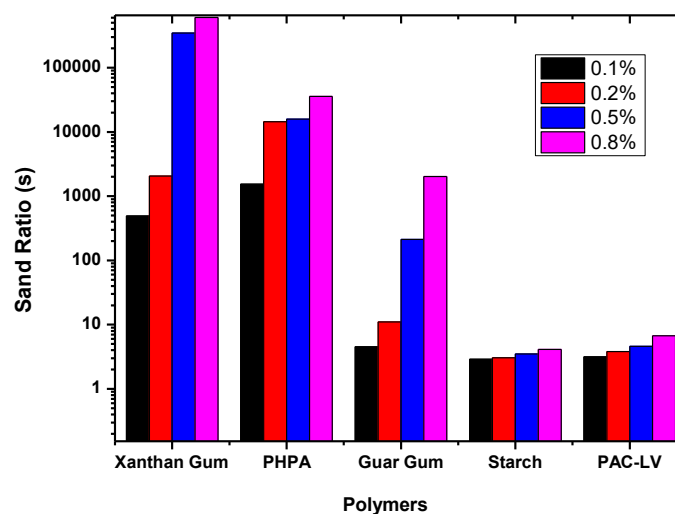


Figure 11: Settling rate for all concentrations of the polymers for sand ratio settling tests

### 3.3 Drag Reduction Rates Performance

In this study, we assess drag reduction rates by varying flow rates (from 20L/min to 75L/min in 5L/min increments) for different concentrations (0.1%, 0.2%, 0.5%, and 0.8%) of friction-reducing polymers. Additionally, experiments are conducted at temperatures ranging from 86 °F to 158 °F (in 18 °F intervals) for each polymer. Drag reduction rates in pipelines can be estimated by measuring the pressure drop along the length of the pipeline. The pressure drop with the presence of the friction reducer (test fluid) is compared to the pressure drop without the friction reducer (based fluid). This can be done by using pressure transducers or gauges at different points along the pipeline to measure the changes in pressure.

The curve profiles for drag reduction rates of polymers with flow rates typically show a non-linear relationship. For instance, as shown in **Figure 12** for 0.1% conc of Xanthan Gum, at low flow rates, the drag reduction rate is generally low, as the flow rate increases, the drag reduction rate also increases for all the temperature intervals. However, as the flow rate continues to increase, there may reach a point where the drag reduction rate plateaus or even decreases as in the case of drag reduction rates for 86 °F. The flow rate of a fluid can have a direct impact on the effectiveness of drag reduction rates.

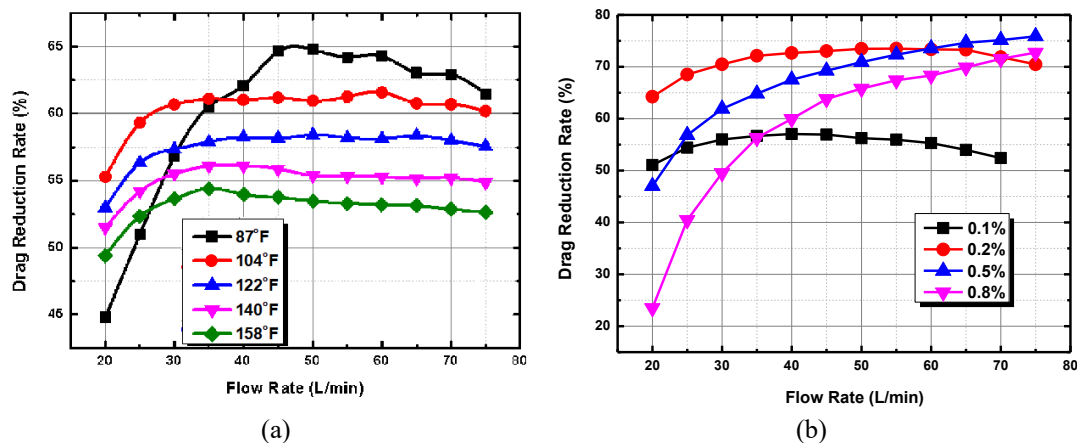
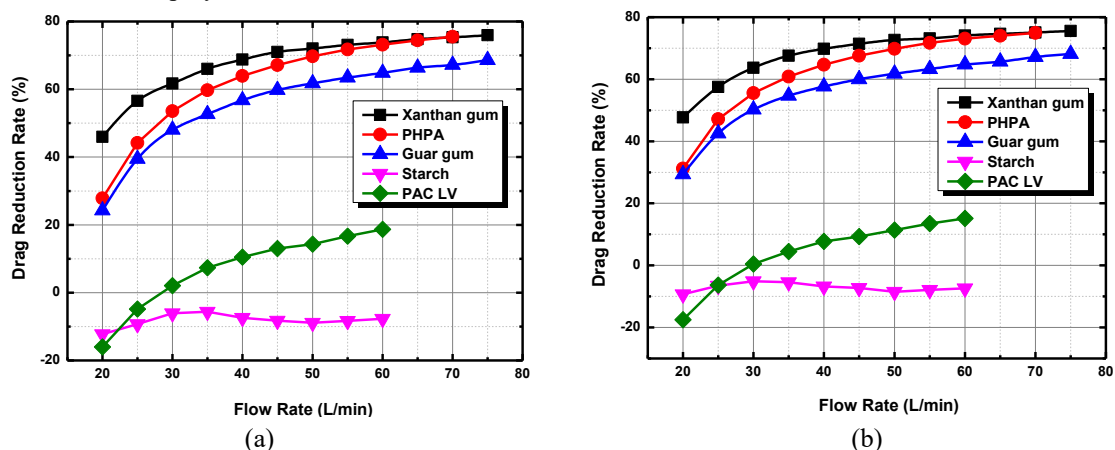
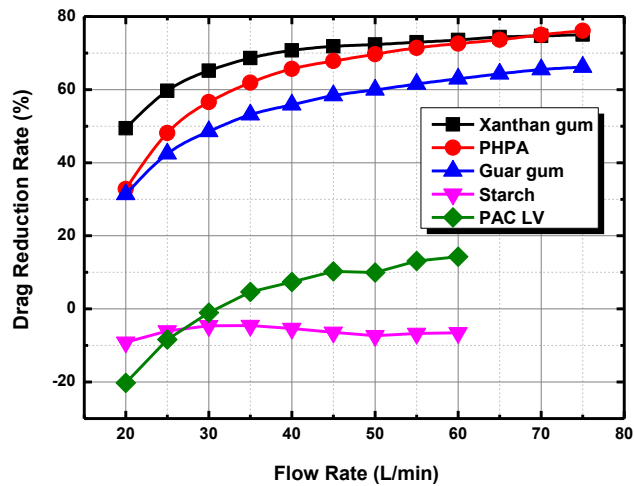


Figure 12. (a) Drag reduction rates for 0.1% concentration of Xanthan Gum at different temperatures (b) Effect of concentrations on drag reduction rates @ 86°F in 10mm pipe diameter for Xanthan Gum

When it comes to drag reduction, increasing flow rates and higher temperatures can sometimes lead to better performance of drag reduction techniques. This is because higher temperatures and flow rates can help to distribute the friction reducers more evenly throughout the fluid most especially at higher concentrations, leading to more effective drag reduction. On the other hand, excessively high flow rates can sometimes diminish the effectiveness of drag reduction rates. This is because at very high flow rates, the fluid may move too quickly for the additives to have a significant impact on the boundary layer. In these cases, the drag reduction rates may be lower than expected, or the friction reducers may not be able to effectively reduce drag at all. This is mostly observed at low concentrations of the polymers.





(c)

Figure 13. Drag reduction rates for all the polymers at 0.5% concentration in 10mm pipe diameter at (a) 122°F, (b) 140°F and (c) 158°F

It can be observed that the curve profile for Xanthan Gum and PHPA exhibits the highest drag reduction rates around 75% and 78% respectively across the flow rates limitation of the experiments. However, it is shown in **Figure 13(c)** that the rising trend of PHPA at higher flow rates tend to approach higher drag reduction rates than Xanthan Gum. Considering the available data, it is likely that PHPA would outperform Xanthan Gum in terms of friction reduction at elevated temperatures and flow rates. Unfortunately, due to limitations in the pipeline friction loop system in our lab, we cannot exceed 75 L/min flow rates and 158°F temperature. Also, PAC-LV experiences increased polymer degradation at higher temperatures. Additionally, Starch consistently shows negative drag reduction rates across all flow rates. In summary, both Xanthan Gum and PHPA excel in friction reduction, with Xanthan Gum performing better at low flow rates and PHPA outperforming at higher flow rates and temperature.

### 3.4 Salinity Effects on the Polymers

Understanding the impact that field source water chemistry or the influence of salinity on the performance of friction reducers is essential to optimize hydraulic fracturing operations in saline environments, enhance efficiency, and minimize costs. Some of the destabilization processes experienced in these experimental tests are shown in **Figure 14**. The tests are conducted through four different approaches: multi sample stability analyses, TDS measurements, tensiometer testing, and rheological testing.

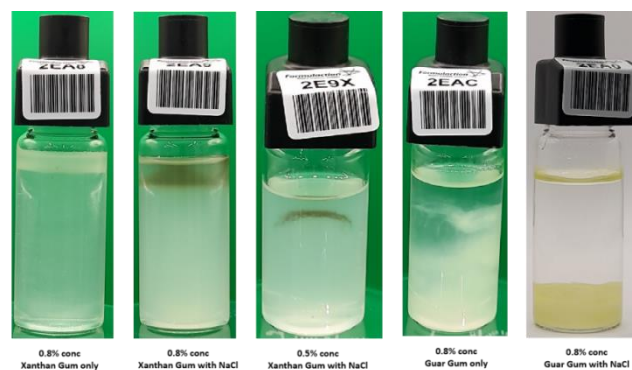


Figure 14. Destabilization processes in some of the prepared samples

#### 3.4.1 Multi-Sample Stability Analyses

Multi-sample stability analysis using Turbiscan Tower is an effective way to evaluate the physical stability of multiple samples simultaneously. This is particularly beneficial when developing new formulations or comparing different product variants to ensure product quality and longevity. The stability of a colloidal system refers to the ability of the colloidal particles to remain dispersed and uniformly distributed within a medium over time, without settling, flocculating, or agglomerating. The multi-sample stability analyses are based on stability curves that demonstrate how the presence and concentration of particles changes over time, aiding to identify whether a formulation is stable, metastable, or unstable. In this section, the stability analyses are based on the interactions and influence of the polymer concentration ions and the NaCl in the base fluid.

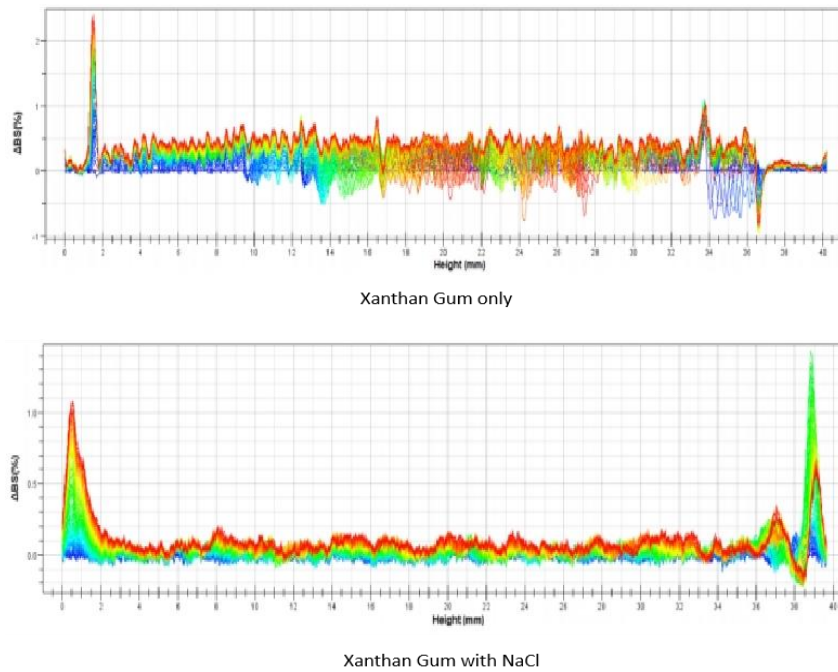


Figure 15: Backscattering signal for 0.2% conc of Xanthan Gum with and without NaCl

Monovalent ion brine, such as sodium chloride (NaCl), can have both positive and negative effects on friction reducers. In the case of Xanthan Gum, the backscattering signals indicate that some particles settled at the bottom (sedimentation) as shown in **Figure 15(a)**. However, some particles settled at the bottom and top of the sample cell when NaCl was added to the solution. It can be inferred that the monovalent ion brine has a negative effect on Xanthan Gum. Though, this negative effect decreases with increase in the concentration of Xanthan Gum. Even so, the NaCl content in this investigation stays constant.

Figure 15 shows the backscattering signals for 0.5% concentration of PHPA. It can be observed that when PHPA only is dispersed in the deionized water, there are lumps scattered from the bottom to the top of the sample as shown with different peaks in Figure 15(a). However, these peaks or spikes of the backscattering signals are suppressed when NaCl is added to the solution and leading to the particles settling at the top of the sample (creaming) as shown in Figure 15(b).

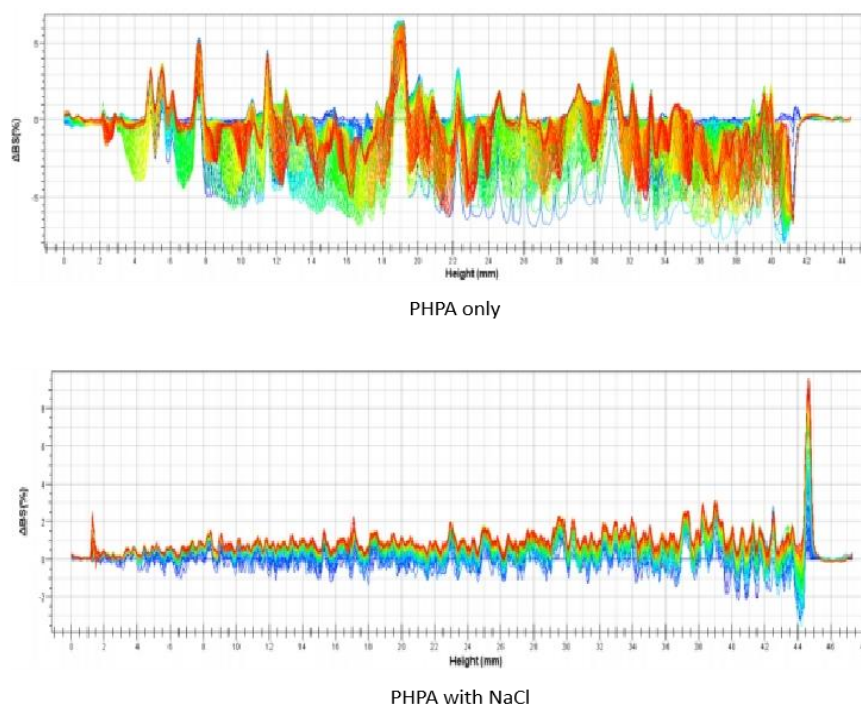


Figure 16: Backscattering signal for 0.5% conc of PHPA

The backscattering flux increases at the top of the sample due to an increase in the concentration of the dispersed phase. It can be inferred that the monovalent ion brine has a positive effect on PHPA. This is as a result of high level of destabilization in the sample with PHPA only which is significantly suppressed when monovalent ion brine is added to the sample. The degree of destabilization in PHPA sample in a standalone form increases as the concentration increases.

The shape of the backscattering curve can provide qualitative information about the particle size distribution. Peaks or shifts in the distribution can indicate broader size ranges or the formation of larger aggregates. However, another quantitative measures that can be used to assess the stability of the samples colloidal dispersions is Turbiscan Stability Index (TSI). The TSI is calculated based on the transmission and backscattering profiles at various depths of the sample over time. It represents the overall stability of the colloidal system, with a lower TSI indicating greater stability.

It can be deduced from **Figure 17** that there is a significant increase in the TSI values when NaCl is added to Xanthan Gum sample. Indicating that Xanthan Gum becomes moderately and physically unstable when interacting with the monovalent ion brine. However, the TSI values for PHPA decreases from around 5.5 to 2 indicating and supplementing the observation in the backscattering signal for the same PHPA that there are possibilities that the monovalent ion brine has positive effects and may improve the physical stability of the polymer. It can also be noted that there are only minor relative changes in the TSI values for Guar Gum sample, both in its standalone form and when NaCl is added which suggests that the particle size and distribution within the samples are not changing significantly.

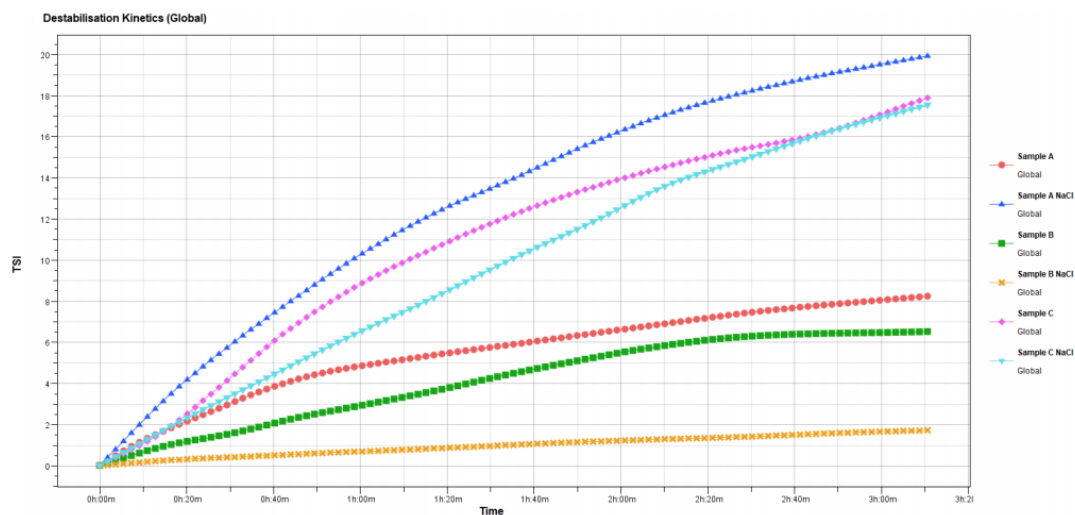


Figure 17: Turbiscan Stability Index (TSI) for 0.1% conc of Xanthan Gum, PHPA and Guar Gum

### 3.4.2 Influence of Salinity from Rheological Measurements

As salinity increases, the viscosity of polymer solutions can change due to alterations in the molecular structure and interactions. Higher salt concentrations often lead to a reduction in viscosity because ions can screen the electrostatic repulsion between charged polymer chains, allowing them to approach more closely and become less entangled. The presence of salts can shift the transition between different flow regimes, affecting the apparent viscosity and yield stress. Salinity may modify the extent of shear thinning by altering polymer layering and interactions. **Figure 17** illustrates the shear thinning characteristics of 0.1% concentration of PHPA, both with and without the presence of NaCl.

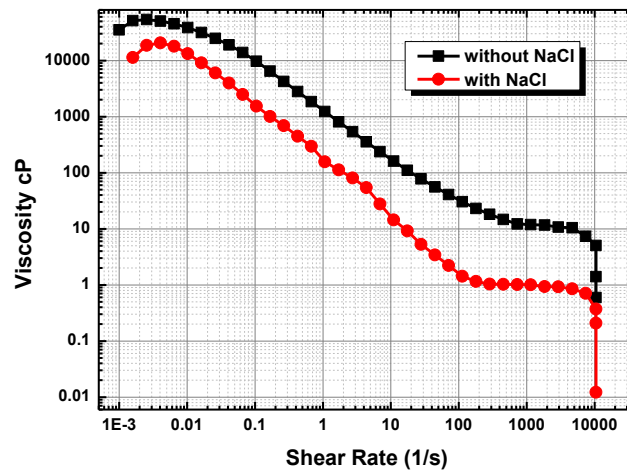


Figure 17: Shear thinning characteristics of 0.1% conc PHPA

Based on Figure 17, it can be observed that the inclusion of monovalent ion brine induces reduction in the viscosity of the polymers and there are shifts in the transition between the flow regimes, affecting the apparent viscosity and yield stress. In addition, the extent of shear thinning is modified by the presence of NaCl in the polymers. However, Figure 17 shows that PHPA exhibits greater sensitivity to monovalent ion brine at this concentration compared to Xanthan Gum, as evidenced by the variations in the shear thinning slope and the transition between low and high shear rates.

The ideal viscosity can vary based on the specific conditions of the wellbore, the type of fluid used, and the properties of the formation. Generally, the best viscosity range for friction reducers in hydraulic fracturing is typically around 10 to 100 cP (centipoise) at the shear rates encountered during fracturing operations. The linear shear rate of 0.2% concentration of PHPA is illustrated in Figure 18.

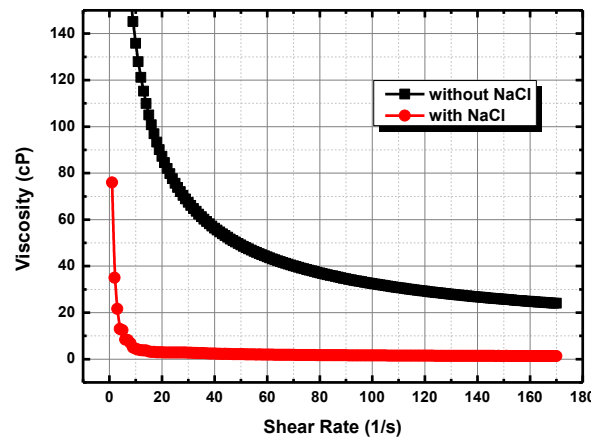


Figure 18: Linear Shear Rate of 0.2% concentrations of Xanthan Gum

### 3.4.3 Molecular Mechanisms Governing Polymer Stability in Saline Environments

The differences in stability observed in the Turbiscan and TSI measurements arise from distinct polymer-ion interactions that affect chain conformation and network formation. Xanthan Gum destabilization in NaCl solutions is attributed primarily to charge screening, conformational collapse, and salt-induced phase separation. The high density of carboxylate groups along the Xanthan side chains is significantly screened by  $\text{Na}^+$  ions, which reduces repulsive forces between chains and allows them to collapse into more compact structures. This collapse decreases the hydrodynamic volume of each polymer chain and leads to reduced viscosity, faster sedimentation, and the creaming observed in the backscattering profiles. At sufficiently elevated ionic strength, monovalent salts can also induce salting-out behavior in polysaccharides, resulting in the formation of polymer-rich and polymer-poor phases, consistent with the observed destabilization phenomena.

PHPA, in contrast, displays improved stability at lower NaCl concentrations due to its moderate charge density and flexible backbone structure. Low levels of  $\text{Na}^+$  partially suppress intra-chain hydrogen bonding and electrostatic interactions, enabling PHPA coils to extend more uniformly and reducing the formation of aggregated lumps. This behavior explains the decrease in TSI values for PHPA in the presence of NaCl. However, at higher PHPA concentrations, the same charge-screening mechanism can promote

inter-chain association, potentially leading to flocculation. This trend aligns with the increased destabilization observed at higher PHPA loadings.

Guar Gum, Starch, and PAC-LV exhibit limited sensitivity to monovalent salts because their interactions are dominated by hydrogen bonding rather than electrostatic repulsion. As a result, their structural changes in NaCl primarily reflect modifications to hydration and water activity rather than direct ion-binding effects.

While this study focuses on NaCl to isolate monovalent ion effects, it is recognized that divalent cations such as  $\text{Ca}^{2+}$  and  $\text{Mg}^{2+}$  commonly present in formation waters may induce stronger polymer-ion bridging, crosslinking, and precipitation. These interactions are likely to exacerbate destabilization in anionic polymers and will be investigated in future work to further enhance field applicability under realistic brine compositions.

#### 4.0 FIELD-SCALE APPLICABILITY AND OPERATIONAL CONSIDERATIONS

Although the present work was conducted under controlled laboratory conditions, the testing methodology is designed to be scalable to field operations. In the field, rheological properties of the fracturing slurry are measured continuously using flow meters, pressure transducers, and dedicated software (e.g., FracPro). These instruments provide real-time pressure-transient data along the entire wellbore, enabling operators to adjust the fluid formulation on-site to maximize carrying capacity while minimizing friction. The laboratory protocol can be coupled with the same instrumentation, allowing seamless translation of the test results to in-situ monitoring and facilitating rapid feedback during fracturing operations.

The pipeline friction loop reproduces representative Reynolds numbers encountered in hydraulic fracturing and pipeline transport, enabling direct extrapolation of drag reduction behavior. Rheological fingerprints obtained from amplitude and frequency sweeps can be used to predict polymer behavior under field-relevant pressure pulsations and flow variations. Salinity and stability measurements using Turbiscan and TSI also provide critical screening tools for selecting polymers suitable for produced-water applications.

The main limitations of the current setup include temperature and flow-rate constraints, single-phase flow, and the use of only monovalent salts. Future work will incorporate multiphase flow conditions, divalent brines, and extended mechanical degradation testing to more closely simulate downhole environments. The methodology can be adapted for real-time monitoring through inline pressure-drop measurements, optical backscattering sensors, and portable rheological tools, offering a pathway for in-situ evaluation and field optimization of friction reducers.

#### 5.0 CONCLUSION

This study reported a performance-based evaluations conducted on the rheological properties, drag reduction rates and performance of various friction reducers aimed at developing a testing methodology for these additives in upstream and downstream applications. The assessments covered four critical areas: rheological property testing, static sand/proppant carrying capacity, drag reduction efficiency in pipeline systems, and the influence of salinity on friction reducer performance.

In this study, comprehensive rheological tests were conducted on the five friction reducers, Xanthan Gum, PHPA, Guar Gum, Starch, and PAC-LV, to evaluate their performance indices. Key parameters like viscosity, shear rate, yield stress, and flow transition indexes were assessed, revealing that all polymers displayed pseudoplastic behavior, reducing viscosity under shear. Increased polymer concentrations enhanced performance, particularly for Xanthan Gum and PHPA, with Xanthan Gum demonstrating superior sand-carrying capability at concentrations of 0.5% and 0.8%. Subsequent evaluations in a pipeline friction loop system revealed a classic bell-shaped drag reduction profile related to flow rates. Xanthan Gum reached a maximum drag reduction rate of 76% at 0.5% concentration, while PHPA achieved 78% at 0.1%. Conversely, Starch and PAC-LV delivered unsatisfactory results. The final phase assessed the influence of salinity on friction reducers, using deionized water and monovalent ion brine (NaCl). Findings indicated that salinity negatively impacted the physical stability of Xanthan Gum while enhancing the stability of PHPA, with Guar Gum largely unaffected. Moreover, NaCl reduced the viscosity of both Xanthan Gum and PHPA, particularly PHPA at higher concentrations and altered the surface tension of the polymers. These findings emphasize the necessity of tailoring friction reducer formulations to specific salinity conditions for optimal performance.

The findings from this multi-phase project emphasize the necessity for detailed testing to tailor formulations for specific applications, enhancing overall efficiency in fluid flow management. Future research is essential to grasp the underlying impacts of salinity concentrations and ions on these polymers fully, aiming to develop specialized solutions suited for the diverse environmental conditions encountered in field applications.

## REFERENCES

- [1] C. T. Montgomery, M. B. Smith, *Journal of Petroleum Technology* 2010, 62, 26.
- [2] G. E. King, in *SPE Hydraulic Fracturing Technology Conference*, SPE: The Woodlands, Texas, USA, 2012, p SPE.
- [3] R. Barati, J. Liang, *J of Applied Polymer Sci* 2014, 131, app.40735.
- [4] S. Al-Hajri, B. M. Negash, M. M. Rahman, M. Haroun, T. M. Al-Shami, *ACS Omega* 2022, 7, 7431.
- [5] W. Qingzhi, S. Wang, X. Duan, Y. Li, F. Wang, X. Jin, *Journal of Natural Gas Science and Engineering* 2016, 33, 70.
- [6] W. Xiong, K. Shen, Q. Ba, Y. Liu, H. Zhou, *Energy Science & Engineering* 2021, 9, 1568.
- [7] T. C. Ross, P. Guraieb, S. Graham, C. Yan, N. Ghorbani, T. Hanna, C. Cooper, *SPE Hydraulic Fracturing Technology Conference and Exhibition* 2017.
- [8] Z. Rixing, H. Nasr-El-Din, X. Jin, J. J. Wu, L. M. Pérez, *Improv Oil Gas Recover* 2019.
- [9] G. A. Al-Muntasheri, *SPE Production & Operations* 2014, 29, 243.
- [10] Toms, Be A, in *1st Intl Congr. Rheol.*, 1949, Vol. 2, pp 135.
- [11] E. D. Burger, W. R. Munk, H. A. Wahl, *Journal of Petroleum Technology* 1982, 34, 377.
- [12] M. Ba Geri, A. Imqam, R. Flori, in *SPE Oklahoma City Oil and Gas Symposium*, SPE: Oklahoma City, Oklahoma, USA, 2019, p D021S004R001.
- [13] D. Mowla, A. Naderi, *Chemical Engineering Science* 2006, 61, 1549.
- [14] A. A. Mohsenipour, R. Pal, *Can J Chem Eng* 2013, 91, 190.
- [15] Y. Bo, J. Zhao, J. Mao, H. Tan, Y. Zhang, Z. Song, *Journal of Natural Gas Science and Engineering* 2019, 62, 302.
- [16] M. H. Iqbal, I. A. Hussein, H. I. A. Wahhab, M. B. Amin, *J of Applied Polymer Sci* 2006, 102, 3446.
- [17] T. T. Palisch, M. C. Vincent, P. J. Handren, *SPE Production & Operations* 2010, 25, 327.
- [18] M. Gojko, T. Theriot, H. Linnemeyer, M. Solano, M. Fuller, S. Han, A. Kim, N. N, K. D.H., M. T, D. V., in *SPE Improved Oil Recovery Conference*, 2022.
- [19] E. Nourafkan, M. A. Haruna, J. Gardy, D. Wen, *J of Applied Polymer Sci* 2019, 136, 47205.
- [20] M. Nigel, L. Fernández, F. Barceló, H. Spikes, *Tribology Letters* 2018, 66, 1.
- [21] F. H. Gaskins, W. Philippoff, *J. Appl. Polym. Sci.* 1959, 2, 143.
- [22] W. Michal, G. Mishuris, P. Papanastasiou, *International Journal of Engineering Science* 2021, 158, 103.
- [23] B. A. Mostafa, F. F. Assaad, *J of Applied Polymer Sci* 2008, 107, 732.
- [24] M. Hojczyk, O. Weichold, *J of Applied Polymer Sci* 2011, 119, 565.
- [25] N. S. Shah., A. Vyas, *SPE Production & Operations* 2011, 26, 55.
- [26] B. Ghith, A. Imqam, *SPE Journal* 2022, 27, 60.
- [27] L. Meng, D. Wu, A. Kelly, M. Woodhead, Y. Liu, *J of Applied Polymer Sci* 2016, 133, app.43459.
- [28] I. T. Ebenezer, G. Z. Chen, *International journal of low-carbon technologies* 2014, 9, 157.
- [29] P. Om, A. Padaria, A. Gupta, B. Rangunathan, S. V. Kumar, in *International Conference on Advances in Water Treatment and Management*, Singapore, 2023.
- [30] W. Lei, D. Wang, Y. Shen, X. Lai, X. Guo, *Journal of Polymer Research* 2016, 23, 235.
- [31] Wei, Juanming, Wenfeng Jia, Luo Zuo, Hao Chen, Yujun Feng., *Molecules* 2022, 27, 351.
- [32] Wu, Zhiwei, Xiang'an Yue, Tao Cheng, Jie Yu, Heng Yang, *Journal of Petroleum Exploration and Production Technology* 2014, 4, 9.
- [33] K. M. Knauer, G. Brust, M. Carr, R. J. Cardona, J. D. Lichtenhan, S. E. Morgan, *J of Applied Polymer Sci* 2017, 134, app.44462.
- [34] Ge, Xiaojing, Abdulmohsin Imqam, *SPE Journal* 2023, 28, 876.
- [35] M. Marudova-Zsivanovits, N. Jilov, E. Gencheva, *J of Applied Polymer Sci* 2007, 103, 160.